Biogeochemistry **68:** 71–105, 2004.

Pre-industrial and contemporary fluxes of nitrogen through rivers: a global assessment based on typology

PAMELA A. GREEN[1,*], CHARLES J. VÖRÖSMARTY[1,2], MICHEL MEYBECK[3], JAMES N. GALLOWAY[4], BRUCE J. PETERSON[5] and ELIZABETH W. BOYER[6]

*[1]Water Systems Analysis Group, Institute for the Study of Earth, Oceans, and Space, University of New Hampshire, Durham, New Hampshire, USA; [2]Department of Earth Sciences, University of New Hampshire, Durham, New Hampshire, USA; [3]UMR Sisyphe, Université de Paris VI, Paris, France; [4]Department of Environmental Sciences, University of Virginia, Charlottesville, VA, USA; [5]Ecosystems Center, Marine Biological Laboratory, Woods Hole, MA, USA; [6]State University of New York, College of Environmental Science and Forestry, Syracuse, NY, USA; *Author for correspondence (e-mail: pam.green@unh.edu; phone: +1-44-603-862-4208; fax: +1-44-603-862-0587)*

Received 24 March 2003; accepted in revised form 11 August 2003

Key words: Anthropogenic loading, Global, Nitrogen, Nitrogen budget, Nitrogen yields, Rivers, Watershed

Abstract. This paper provides a global synthesis of reactive nitrogen (Nr) loading to the continental landmass and subsequent riverine nitrogen fluxes under a gradient of anthropogenic disturbance, from pre-industrial to contemporary. A mass balance model of nitrogen loading to the landmass is employed to account for transfers of Nr between atmospheric input sources (as food and feed products) and subsequent consumer output loads. This calculation produces a gridded surface of nitrogen loading ultimately mobilizable to aquatic systems (Nmob). Compared to the pre-industrial condition, nitrogen loading to the landmass has doubled from 111 to 223 Tg/year due to anthropogenic activities. This is particularly evident in the industrialized areas of the globe where contemporary levels of nitrogen loading have increased up to 6-fold in many areas. The quantity of nitrogen loaded to the landscape has shifted from a chiefly fixation-based system (89% of total loads) in the pre-industrial state to a heterogeneous mix in contemporary times where fertilizer (15%), livestock (24%) and atmospheric deposition (15%) dominate in many parts of the industrialized and developing world. A nitrogen transport model is developed from a global database of drainage basin characteristics and a comprehensive compendium of river chemistry observations. The model utilizes constituent delivery coefficients based on basin temperature and hydraulic residence times in soils, rivers, lakes and reservoirs to transport nitrogen loads to river mouths. Fluxes are estimated for total nitrogen, dissolved inorganic nitrogen, and total organic nitrogen. Model results show that total nitrogen fluxes from river basins have doubled from 21 Tg/year in the pre-industrial to 40 Tg/year in the contemporary period, with many industrialized areas of the globe showing an increase up to 5-fold. DIN fluxes from river basins have increased 6-fold from 2.4 Tg/year in the pre-industrial to 14.5 Tg/year in the contemporary period. The amount of nitrogen loading delivered to river mouth as flux is greatly influenced by both basin temperatures and hydraulic residence times suggesting a regional sensitivity to loading. The global, aggregate nitrogen retention on the continental land mass is 82%, with a range of 0–100% for individual basins. We also present the first seasonal estimates of riverine nitrogen fluxes at the global scale based on monthly discharge as the primary driver.

Introduction

A wide array of human activities is accelerating the natural fluxes of reactive nitrogen (Nr) through river basins and over the continuum of aquatic transport routes into the coastal zone where land-based activities generating point and non-point sources in upstream watersheds have been implicated (Jordan et al. 1997; Russell et al. 1998; Pionke et al. 1999; Hession et al. 2000; Goolsby and Battaglin 2001). The evidence of nitrogen pollution is ubiquitous and can be seen in individual small watersheds (Hopkinson and Vallino 1995), regional to continental drainage systems (Howarth et al. 1996; Jordan et al. 1997; Russell et al. 1998; Pionke et al. 1999; Hession et al. 2000; Goolsby and Battaglin 2001), and now even global-scales (Seitzinger et al. 2002a; Galloway et al. 2003). Associated with these elevated Nr fluxes are enhanced coastal eutrophication and anoxia (Turner and Rabelais 1994), changes in nutrient stoichiometry (Mackenzie et al. 1993; Ver et al. 1999) that possibly favor toxic phytoplankton (Justic et al. 1995), and increases in the production of greenhouse gases (Kroeze and Seitzinger 1999). Human induced changes to the nitrogen cycle therefore have far-field impacts with respect to pollution and public health, protein supply for humans, and planetary heat balance. At the same time, land-to-ocean fluxes in earth system models have remained poorly articulated and we are only now beginning to develop the synthetic perspective necessary to address the complex outcomes of the acceleration of Nr loading (Hobbie 2000; Vörösmarty and Peterson 2000). There is a major need for data sets and models to understand the primary factors regulating mobilization, processing, and transport of constituents through the full continuum of airshed–land–inland aquatic systems from source area to ocean (Billen and Garnier 1999; Alexander et al. 2000).

This paper is a contribution to emerging work that simulates the distribution of fluxes of geochemical constituents across river basins to receiving waters (e.g., Ludwig and Probst 1996, 1998; Vörösmarty et al. 1997a,c, 2003; Seitzinger et al. 2002a; Galloway et al. 2003) in a consistent and geographically-specific manner. Such studies have combined a number of geospatial, global, biogeophysical data sets with relatively simple models to predict a spatially varying flux of material delivered from the land to the coastal zones of the world. Many of these studies have estimated total nitrogen loading within a river basin as the sum of the atmospheric inputs (deposition, fixation, industrial fertilizer) as well as land based consumer loads (human and livestock emissions), but without accounting for intermediate transfers of Nr between atmospheric input sources, essentially as food and feed products, and subsequent consumer output loads (Caraco and Cole 1999; Seitzinger et al. 2002a). This approach results in a double counting of Nr loading available for transport to river outlets. In those cases where an accounting of mass balance has been applied (Howarth 1998; Boyer et al. 2002; Howarth et al. 2002), adjustments where made for net import or export of Nr in food and feed on a watershed basis but were not articulated as a spatially distributed surface of nitrogen loading. A few recent studies have begun to include an accounting of mass balance of Nr inputs to the landscape at the global scale including all major at-

mospheric inputs (fixation, deposition, industrial fertilizer), denitrification, ammonia volatilization, losses due to biomass burning and natural soils emissions, and transfers through food and feed import/export (Van Drecht et al. 2001; Galloway et al. 2003). The current analysis presents a consistent and mass balanced methodology to estimate Nr loading to the landmass and aquatic systems in a spatially distributed and detailed manner. The method accounts for the major losses, transfers and storages of Nr for the discharging landmass of the globe. Comprehensive work including detailed components of the nitrogen cycle has also been carried out at the individual basin and smaller regional domains (Jordan et al. 1997); however, these analyses were not designed to be scalable to the global domain and are of limited use outside of the regions to which they were originally applied. The analysis presented in our paper provides a methodology for estimating nitrogen loads and fluxes at the global scale that can be directly used in global change studies.

The overall objective of this study is to provide a global synthesis of our current understanding of Nr loading to the continental landmass and subsequent riverine Nr fluxes under a gradient of anthropogenic disturbance, from pristine to highly industrialized. We consider separately atmospheric Nr deposition, industrial fertilization, and fixation and their subsequent redistribution across the continental landmass. This redistribution results from the interception of atmospheric Nr inputs by (a) the growth, harvesting and transport of crops for human consumption, (b) the growth, harvesting and transport of feed and forage for livestock, (c) the production and transport of animal products, and the losses of Nr through (i) ammonia volatilization from fertilizer, (ii) emission from livestock, (iii) removal by sewage treatment systems, and (iv) natural emissions from soils and biomass burning. We have assumed for this work that potential exports are equal to atmospheric inputs across natural ecosystems and managed forests though we recognize that this needs further elaboration (Jaworski et al. 1997). Losses due to denitrification and sequestration in soils and plants are estimated by difference using a basin-scale constituent transport model. Our goal is to develop a global database of Nr loading to the landmass that preserves mass balance while at the same time allowing us to map with a high degree of spatial specificity reflecting the distributed nature of these loadings.

A constituent transport model is developed using a newly assembled global data base of drainage basin characteristics together with a comprehensive compendium of river chemistry observations analyzed in the context of a river basin typology scheme which permits us to extrapolate nitrogen river flux estimates from a set of well-monitored rivers to unmonitored rivers. Our method presented here includes coefficients for transport of nitrogen through river networks, lakes, reservoirs and soils at the global scale based on basin temperature and water residence time providing a comparison of the differentiated transport mechanisms within river basins. Some previous studies have included analysis of nitrogen retention along flow paths but these have been for individual basins or regions (Alexander et al. 2000; Seitzinger et al. 2002b). We provide flux estimates for the entire discharging portion of the continental landmass at $30'$ spatial resolution (longitude $\times$ latitude)

for Nr partitioned into dissolved inorganic nitrogen (DIN), total organic nitrogen (TON), and total nitrogen (TN). We also provide estimates of global, continental, regional, and coastline-specific estimates of Nr loadings onto the continental landmass, the efficiency of transformation of land-based loadings into riverine flux for different parts of the world, the riverine nitrogen fluxes themselves, and an estimate of the errors associated with these fluxes. Finally, we produce the first global, time-varying inputs of TN to the world's coastal zone, simulating a seasonal climatology that is of potential value in improving our understanding of coastal ecosystem dynamics. Nitrogen river fluxes are developed for the pre-industrial and contemporary (mid-1990) conditions.

Methods

Overall strategy

A global database of nitrogen loading to the landmass is developed which preserves mass balance against all known, major inputs while at the same time mapping the distributed nature of the nitrogen inputs with a high degree of spatial specificity. Derivation of the distinct sources of mobilizable nitrogen loads and their redistribution across the landmass are described in '*Nitrogen loading to the landmass*'. The mobilizable loads of nitrogen to the landmass in conjunction with key river basin characteristics are used as inputs to a Constituent Transport Model (CTM) to develop estimates of TN, DIN and TON fluxes at river mouths for the globe. The CTM described in '*Estimation of nitrogen fluxes at basin mouth*' is based on statistical relationships linking biophysical characteristics of drainage basins to observed constituent fluxes providing global, continental, regional and coastline-specific estimates of organic and inorganic mouth-of-basin fluxes in both pre-industrial and contemporary conditions. The statistical relations attempt to incorporate both hydrologic and metabolic controls on the nitrogen riverine fluxes.

Nitrogen loading to the landmass

The mass balance model of Nr loading depicted in Figure 1 introduces the concept of atmospherically derived sources of Nr that are spatially distributed across the landmass including water bodies and ultimately mobilizable to aquatic systems (Nmob). In the contemporary state the mass balance model accounts for the atmospheric inputs of Nr in the form of deposition, industrial fertilizer application and fixation and their subsequent lateral redistribution across the landmass as a function of the growth, harvesting and transport of feed and forage for livestock production and of crops and livestock for human consumption. This redistributed atmospheric Nr is reintroduced to the landmass at the receiving point in the form of animal and human waste products. At any point on the landmass, Nmob is de-

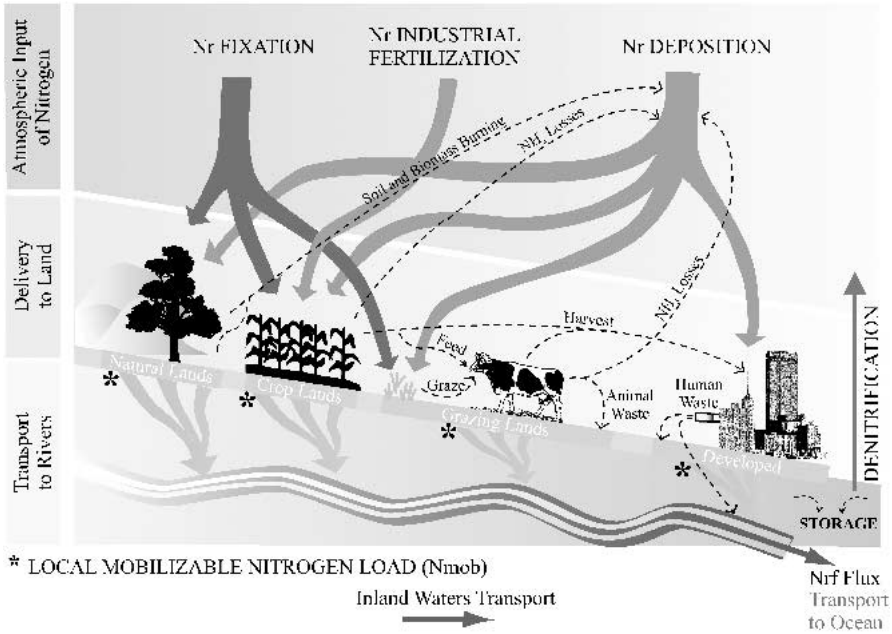

Figure 1. Overall computation scheme showing the major sources of reactive nitrogen (Nr) loaded onto the continental landmass locally that are then redistributed spatially through food and feed trade. A mass-conserving approach is applied with initial loadings tracked and reconstituted as mobilizable loads (Nmob) to inland aquatic systems. Mobilizable loads are diminished relative to the original Nr due to denitrification losses on land and in aquatic systems and potential sequestration. These inferences on loss are derived from non-linear statistical models of TN and DIN that simulate a sequential efficiency of transport based on hydraulic residence time and temperature.

termined by the addition of Nr atmospheric sources, but decremented by the lateral redistribution of Nr that takes the form of subsequent human and animal waste loading in the contemporary state. For the pre-industrial state (conditions prior to 1800 c.e.) we consider all atmospheric sources of Nmob to be loaded and transformed to animal and human wastes locally within each grid cell, assuming long distance lateral transports of food and feed products for this period are negligible. Therefore, we regard the atmospheric loads of nitrogen in the form of fixation and deposition within in each grid cell to serve as the net Nmob loading to the land mass for the pre-industrial state. We have assumed for this work that potential exports are equal to Nr atmospheric inputs at the grid cell scale across natural ecosystems and managed forests for both the pre-industrial and contemporary states. Sequestration and losses due to denitrification will therefore be articulated by difference from the basin-scale semi-empirical CTM of Nmob flux described in '*Estimation of nitrogen fluxes at basin mouth*'. Both pre-industrial and contemporary loads of nitrogen to the landmass are considered and described in the following section.

Spatially distributed data sets

Table 1 lists the sources of the spatially distributed, nitrogen load estimates used in this analysis. All fields for Nr loading and Nmob were derived from original source resolutions (1 km to 1° grids and country level statistics), and then redistributed based on a rule-based system described in the following sections to individual 1 km calculation units. They were then resampled onto a 1 km grid resolution for processing, with the final products resampled to 30′ (longitude × latitude) spatial scale. Following is a detailed description of the derivation of these data sets.

Pre-industrial data sets

Atmospheric nitrogen deposition

Atmospheric inputs for pre-industrial nitrogen deposition were based on modeled estimates of total (wet + dry) inorganic (NO_y plus NH_x) deposition based on a global atmospheric transport model described in Dentener and Crutzen (1994). Original data sets at 1° resolution were resampled to 1 km and 30′ resolution using bilinear interpolation to maintain consistency with other data sets.

Nitrogen fixation

The pre-industrial Nr fixation field was developed from potential rates defined for undisturbed vegetation classes (Cleveland et al. 1999; A. Townsend, personal communication). These rates were applied to a 30′ resolution gridded data set of undisturbed vegetation (Mellilo et al. 1993) to create the distributed pre-industrial Nr fixation data layer.

Contemporary data sets

Atmospheric nitrogen deposition

Atmospheric inputs for contemporary nitrogen deposition were based on modeled estimates of total (wet + dry) inorganic (NO_y plus NH_x) deposition estimates from Dentener and Crutzen (1994). Original data sets at 1° resolution were resampled to 1 km and 30′ resolution using bilinear interpolation to maintain consistency with other data sets.

Nitrogen fixation

The contemporary Nr fixation field includes natural rates for undisturbed systems derived from the pre-industrial Nr fixation layer overlaid by rates for crop, cultivated grasslands and urban areas (Smil 1999 and our own assessment). The crop fixation geospatial field was based on country-level estimates of crop area (FAO 2001) and fixation rates for the predominant Nr fixing crops (seed legumes, open fields, rice, and sugar cane) (Smil 1999). These rates were evenly applied across a 1 km data set of contemporary cropland (EDC 2000) within each country. Since

Table 1. Spatially distributed, biophysical data sets used in this analysis. All fields were resampled to 30′ (longitude × latitude) spatial scale.

Biophysical parameter	Original spatial resolution	Source/archive
Nitrogen loading (converted into N equivalents) from:		
N deposition (NO_y and NH_x)	5°	Dentener et al. (1994)[1]
N fixation		
Pre-industrial	30′	Cleveland et al. (1999); A. Townsend (personal comm.)[1,2]; Melillo et al. (1993)[3]
Contemporary	1 km, country statistics, 30′	EDC (2000); FAO (2001)[4]; Natural fixation from pre-industrial
Fertilizer use/input	1 km, country statistics	EDC (2000); FAO (2001)[4];
Livestock	1°, country statistics	Lerner et al. (1989); FAO (2001)[5]
Human population	1 km, country statistics	Vörösmarty et al. (2000); FAO (2001); WRI (1998); UN (1998); OECD (1999)[6]
Surface hydrology attributes		
River networks and watershed boundaries (STN30 v5.12)	30′	Vörösmarty et al. (2000)
Discharge and runoff (annual and monthly)	30′	Fekete et al. (1999)[7]
Soil moisture (annual and monthly)	30′	Fekete et al. (1999)[7]
Lake density and volume	Vector (1:1M)	ESRI (1992)
Reservoir induced aging	Basin scale	Vörösmarty et al. (1997)[8]

Table 1. (continued)

Biophysical parameter	Original spatial resolution	Source/archive
Land surface attributes		
Air temperature	30′	Willmott and Matsuura (1999)
Precipitation	30′	Willmott and Matsuura (1999)
Potential vegetation	30′	Melillo et al. (1993)[3]
Contemporary land cover	1 km	EDC (2000)

[1]For both pre-industrial and contemporary conditions.
[2]Rate of fixation given as function of vegetation type.
[3]For pre-industrial condition.
[4]Computed from N application rates and distribution of cultivated land (EDC 2000; FAO 2001).
[5]Livestock loads based on FAO (2001).
[6]Calculated on the basis of a per capita N loading and removal by sewerage treatment (UN 1998; WRI 1998; OECD 1999; FAO 2001). This loading was associated with urban and rural populations from Vörösmarty et al. (2000).
[7]Computed from 679 discharge observing stations over 73% of the actively discharging portion of the continental land mass. Remaining fraction of land simulated using the water balance model of Vörösmarty et al. (1998).
[8]Aging at the basin scale calculated as the net storage of impounded water divided by mean annual discharge at river mouth.

little information was available on the spatial distribution of leguminous ground cover on forage and crop lands a global estimate of 12 Tg nitrogen fixation (Smil 1999) was distributed uniformly across a 1 km data set of grazing lands assumed to contain leguminous crop cover and green manures (EDC 2000). We judge the error in this assignment to be small given the relatively minor contribution of this element to the global flux and the generally good visual correlation between cropland and animal population distributions. Where crop and/or leguminous ground cover were present these values were superimposed on the pre-industrial fixation layer. Any pixels containing predominantly urban areas as defined by a city lights data set (Elvidge et al. 1997) were assigned a fixation value of 0. Because an estimate of net fixation is sought here, soil emissions of nitrogen in the form of ammonia (NH_3) were deducted from the fixation estimates for both the natural and contemporary states (1.9 TgN/year globally) (Bouwman et al. 1997). In addition, nitrogen losses from biomass burning, where known to occur, were also deducted from the contemporary fixation field (3.5 TgN/year globally) (Bouwman et al. 1997). The contemporary nitrogen fixation data set was resampled to 30′.

Industrial nitrogen fertilizer application
We computed net fertilizer inputs for the contemporary state accounting for volatilization losses from field-application and manufacturer losses. Fertilizer loads are considered for industrial sources only and no estimation was made for animal manure fertilizers which are included as a part of the livestock waste layer. Country-level nitrogenous fertilizer consumption totals for 1995 were taken from the FAOSTAT Statistical Databases (FAO 2001) to represent the contemporary state. These country-level values were evenly distributed among a 1 km resolution cropland data set (EDC 2000). Each 1 km cropland pixel within a country received an equal fraction of the total fertilizer consumption for that country. We recognize that using a constant fertilizer application rate within a country may introduce errors, particularly in larger countries such as China, Russia, USA, and Brazil, where cropland extent and type may greatly vary. Ammonia volatilization losses from fertilizers can be substantial and were therefore deducted from the fertilizer Nr loads using the regression equation put forth by Bouwman and Boumans (2002). The net fertilizer consumption data set was then resampled to 30′.

Distribution of human waste loads of nitrogen.
Point source loads of nitrogen directly input to river systems were associated with sewered urban population alone. Human loads of nitrogen from rural and urban populations not serviced by sewers were considered as non-point source loads and applied directly to the land. Human waste loads were calculated using total nitrogen intake estimates applied to a 1 km spatially distributed global data set of urban and rural population (Vörösmarty et al. 2000c) and country based sewage rates (WRI 1998). The amount of nitrogen excreted was linked to nitrogen intake in diet derived from protein per capita estimates based on specific crop and animal product type by country in the FAOSTAT database (FAO 2001). Nitrogen intake ranged from 1.7 kg N/person/year in the Democratic Republic of the Congo to 6.9 kg N/

person/year in Iceland with a global average of 4.2 kg N/person/year. Countries lacking dietary protein intake information were assigned an average per capita intake value from a neighboring country of similar economic and dietary make-up. Nitrogen sequestration in growing human populations was estimated by the percentage of nitrogen intake retained for growth using country population growth rates between 1990 and 1995 (FAO 2001).

For populations with access to sewage treatment, the percentage of urban population connected to sewer systems was obtained from WRI statistics and the United Nations Human Settlements Programme on populations connected to public sewage systems (UN 1998; WRI 1998). The level of wastewater treatment for these sewered populations was derived from the OECD statistics for selected countries (OECD 1999). Sewage treatment levels for countries not in the OECD database were extrapolated from data listed for the OECD countries based on a statistical relationship between treatment level and GDP (WRI 1998). Sewered urban populations were assumed to have a 60% removal of total nitrogen through wastewater treatment processes for tertiary treatment (Steel and McGhee 1979; Caraco and Cole 1999), 25% for secondary treatment, and 10% for primary treatment (Steel and McGhee 1979). Globally, 58% of the world's population is connected to sewer systems with 24% receiving some level of sewage treatment (4% primary, 15% secondary and 5% tertiary). Rural and non-sewered urban populations were assumed to have no reduction in nitrogen content of excretion. The point source and non-point source human waste data sets were then resampled to $30'$.

Distribution of animal intake and excretion of nitrogen.
A 1° spatial resolution map of domesticated animals (Lerner et al. 1988) was used to derive the extent of animal uptake of Nr by applying average nitrogen required per animal type based on a range of protein requirements for all animal ages (NRC 1985; Smil 1999). Animal waste load distribution was derived by applying species-specific Nr emission units based on animal intake (NRC 1985; Smil 1999) minus ammonia volatilization (Smil 1999) yielding the following effective nitrogen loads to the land per livestock head: dairy cattle 43.2 kgN/year industrial world and 24.3 kgN/year developing world, non-dairy cattle 30.4 kgN/year industrial world and 18.2 kgN/year developing world, swine 8 kgN/year, sheep and goats 6.5 kgN/year, horses 34.2 kgN/year, caribou and camels 30.6 kgN/year, and water buffalo 28.8 kgN/year (NRC 1985; Smil 1999). Ammonia volatilization rates were taken from Smil (1999) and are 36% for cows and pigs; 28% for goats, sheep, horses, caribou and water buffalo. The cattle classes (dairy and non-dairy) were subdivided into developing and industrialized world classes to reflect differences in lower body weights and poorer feeds in low-income countries. Other livestock animals, such as poultry, were not included in this analysis due to a lack of spatial information at the global scale. However, these excluded animals represent only $\sim 5\%$ of the total global nitrogen loads from livestock (Smil 1999).

We assumed there was a steady state between the harvest and growth of animal stock over the time period. Livestock numbers for domestic livestock animals were updated from the 1984 baseline (Lerner et al. 1988) to 1995 values by determining

the percent increase by country in livestock populations for horses, cattle, pigs, sheep, goats and buffalo from the FAOSTAT database (FAO 2001). It was assumed that no significant change in either camel or caribou populations have occurred over this time frame. Animal intake and excretion were then resampled to the 1 km grid cell scale by distributing the animal equivalents evenly among crop and grazing land (EDC 2000) within each 1° cell. Nitrogen content in the intake and excretion of wild animals was considered to be very small and was not considered in this analysis. The livestock excretion data set was then resampled to $30'$.

Distribution of nitrogen in crops.
The nitrogen content in crops was determined from the country-level production statistics from the FAOSTAT database for 1995. An estimate of the percent of nitrogen in major crop classes was taken from estimates of nitrogen in harvested crops and fresh weight harvest. This was done for seven harvested types globally (cereals, legumes, sugar crops, roots and tubers, vegetables and fruits, forages, and other crops) (Smil 1999). Total nitrogen in crops for each country was calculated as the sum of nitrogen in the individual crops per year for the respective countries. Crop nitrogen content was spatially distributed across all cropland within each country (EDC 2000) weighted by atmospheric inputs to the cropland assuming areas with higher nitrogen input will support greater sequestration in crops. The cropland nitrogen content data set was then resampled to $30'$ resolution.

Distribution of nitrogen in forage and feed for livestock.
Following the determination of estimated livestock intake, a comparison was made between (a) the amount of intake required locally by the animals and (b) what was available both locally through grazing and silage as well as through consumed feeds. The nitrogen content in livestock feed was determined from country level feed statistics based on specific feed crop type in the FAOSTAT database (FAO 2001). Nitrogen content in feed crop classes was defined according to the seven crop group types listed in Smil (1999). Animals on grazing land were given nitrogen in a hierarchical manner by first using locally available grazing land and secondly taking any additional nitrogen sources from the remaining country level feed. Areas where nutritional needs of livestock were not met occur predominantly in developing nations. Since our model does not account for other important feed resources that are difficult to model at the global scale such as animal products (milk mainly), road-side grazing, and household wastes, the amount of nitrogen available for intake may be underestimated in some areas, particularly in developing nations that typically utilize these resources. Noted nutritional deficits may also be due to an overestimation of the nitrogen intake required for livestock in these countries. A single global value was used to represent average intake for each type of animal; therefore, estimations of intake for some countries may be overestimated. In addition, deficits in some countries may be a function of inaccurate reporting of total livestock numbers for the country or incorrect assignment of nitrogen intake values for animals in these areas.

Redistribution of nitrogen loading to the terrestrial and aquatic systems

The mass balance of nitrogen inputs and transfers at the grid cell level yields a spatially distributed surface of nitrogen loadings to the landmass that are potentially mobilizable into river networks. We refer to these loadings, collectively, as Nmob. Nitrogen loads onto the continental landmass are described in the previous section and developed for both pre-industrial and contemporary conditions. Pre-industrial Nmob loadings are considered solely a function of the pre-industrial atmospheric inputs deposition and fixation with no adjustments for lateral transports. The sources of the contemporary 'vertical' nitrogen loading to the landscape include deposition, fixation, fertilizer application, livestock loadings and human loadings. A 'horizontal' component is also present for the contemporary condition, representing the amount of nitrogen taken from grazing lands and harvested croplands and transported as feed (and forage) and as human food consumption. To compute a potentially mobilizable load of atmospheric nitrogen available for aquatic transport, the amount of Nr in food and feed transported out of each grid cell was deducted from the atmospheric inputs of Nr into that grid cell. Where food and feed nitrogen exports from the grid cell exceed inputs into that grid cell, the net mobilizable nitrogen load is set to zero. The adjusted Nmob atmospheric inputs are then added to the gridded distribution of livestock and human Nmob waste loading to derive a spatially distributed surface of contemporary Nmob loadings to the terrestrial and aquatic systems that are potentially mobilizable into river networks.

Estimation of nitrogen fluxes at basin mouth

Much of the globe is unmonitored for both river discharge and water quality. Data from less than 50% of entire landmass and only 72% of the actively discharging portion of the continents provides reliable estimates of river flow (Fekete et al. 1999). For nitrogen these numbers are even more limited with only about 40% of the landmass with relatively reliable data for DIN and 33% for TON (Meybeck and Ragu 1995). To achieve global coverage of nitrogen riverine flux a practical means of extrapolation is necessary.

Our analysis for estimating riverine nitrogen fluxes is based on the typological approach presented by Meybeck (1993) for constituents in river systems. Typology as used here is a means for first characterizing drainage basins based on spatially distributed, geophysical attributes and then applying nutrient flux models to make estimates over unmonitored drainage systems. The flux models are based on relationships linking the biogeophysical characteristics of drainage basins to observed constituent fluxes. Good examples of such an approach using simple multiple regression equations can be found in Kroeze and Seitzinger (1998) for DIN, Ludwig and Probst (1996) for carbon flux, Syvitski et al. (2000) for suspended sediments. The work reported here will explore a statistical model to predict mouth-of-basin fluxes based on full-basin characteristics. The following sections describe the model inputs and derivation.

Data sets

Chemical constituent data

The data set for observed nitrogen flux was taken from the United Nations Environment Program's Global Environmental Monitoring System Global River Inputs (GEMS/GLORI) data set for rivers exceeding 10 000 km^2 drainage area, 10 km^3/year discharge or a population of 5 million people (Meybeck and Ragu 1995, 1997). GEMS/GLORI represents the single largest compendium on global river chemistry and attributes of which we are aware. For the purposes of tabulating land-to-ocean fluxes, the data have already been organized to represent conditions at river mouth. Drainage basins smaller than 25 000 km^2 were not included in the analysis due to geomorphometric constraints associated with the 30 min river network described in '*Spatially distributed data sets*'. A total of 281 and 58 sites provided concentration data to this study on DIN and TN, respectively. An original small number of DIN and TN sites ($n = 112$ and 13, respectively) was available through GEMS/GLORI. We augmented this data by combining other nitrogen elements (i.e., total nitrogen = total Kjeldhal N + nitrate) and by inferring relationships between nitrogen and carbon elements provided in the GEMS/GLORI database (i.e., DON derived from DOC, etc.). Area-specific fluxes or yields were calculated based on constituent concentrations and reported runoff values.

The majority of GEMS/GLORI rivers are from the temperate zone although many additional climatic regions are represented, including sub-tropical, desert, and alpine/tundra systems. Rivers in GEMS/GLORI span the full range of nitrogen status from pristine through highly eutrophic. Concentration values range from 0.01 and 5.3 mg l^{-1} for DIN, with export rates from 0.05 to 2 132 kg N km^2/year. TN concentration values range from 0.35 and 6.09 m l^{-1}, with export rates from 0.95 to 2 443 kg N km^2/year. Though not strictly representing an identical time period, individual data entries within GEMS/GLORI represent yearly average concentrations and are reasonably well harmonized with respect to time domain to depict conditions over the recent past. The data for DIN span 1962 through 1996 with 80% of the entries falling between 1980 and 1992. The TN data set spans 1986 through 1996 with 50% of the entries falling between 1993 and 1995.

Spatially-distributed data sets

A total of 14 individual data sets were assembled or constructed as part of this study (Table 1) including the mobilizable Nmob land loads described in '*Nitrogen loading to the landmass*'. All were geographically co-registered to a 30′ spatial resolution grid and organized into distinct river basins using drainage divides represented in the Simulated Topological Network for potential river flow paths (STN-30p) (Vörösmarty et al. 2000a,b). A total of 6 152 basins was potentially available for land-derived fluxes across 133.1×10^6 km^2 of non-glacierized land area. The actively discharging portion of the landmass constitutes 95.1×10^6 km^2 and 5 362 basins. This river network (STN-30a) was determined using STN-30p flow paths and a threshold of

3 mm/year representing the long-term average minimum upstream runoff required to sustain any significant discharge in river channels over a several year period (Vörösmarty and Meybeck 2003). The STN-30a was then used to derive basin-scale attributes for active drainage systems ranging in size from 25 000 km^2 to $>6 \times 10^6$ km^2 for the Amazon basin. The 25 000 km^2 threshold was chosen based on earlier assessment of the limits to using a 30′ resolution river networking system to depict the geomorphometry of drainage basins (Vörösmarty et al. 2000b). This yielded a discharging landmass of 73.6×10^6 km^2 comprising 387 drainage basins.

Water residence time (τ) and temperature were employed to calculate the efficiency of nitrogen processing within and hence transport through drainage basins. Similar recent studies have also employed residence times as a proxy for estimating nitrogen processing efficiency within river basins and stream reaches (Alexander et al. 2000; Peterson et al. 2001; Wolheim et al. 2001). For each drainage basin, a series of τ values was assigned based on the mean duration of time that water spends within soils and shallow groundwater, river channels, lakes, and reservoirs; deeper groundwater is not considered in this analysis due to lack of information at the global scale. Residence time for nitrogen on the landmass was estimated as the sum of the mean annual volume of water stored as soil moisture and shallow groundwater (from 12 monthly estimates) divided by mean annual basin runoff, based on a global-scale water balance model (WBM) (Vörösmarty et al. 1998; Fekete et al. 2002). Residence time in river channels was calculated as the total volume of channel water (i.e., rectangular cross-section assumed; volume = width × depth × length) derived from the geomorphometric attributes of STN-30 (Vörösmarty et al. 2000b) and theory (Leopold et al. 1964). The volume was then divided by the mean annual discharge at the mouth of each basin. For the globe, we obtained a mean, discharge-weighted residence time in the actively discharging channels of the STN-30a of approximately 14 days, in good agreement to estimates which vary from 16 to 26 days (Covich 1993; Vörösmarty et al. 2000a). In basins with large dams and reservoirs an incremental residence time was computed as the accumulated, effective storage volume divided by the mean annual discharge at the mouth (Vörösmarty et al. 1997a,b, 2003). A total of 633 large reservoirs were employed which yielded a global incremental τ of 31 days; in individual basins incremental τ can exceed years. Likewise, incremental residence time in lakes was calculated as the total volume of lakes contained in a basin divided by mean annual discharge at the mouth of the basin. Documented lake volumes were identified for 87 out of the total natural 6 392 georeferenced lakes with known area used in this study (ESRI 1995; Lerman et al. 1995). The small number of known lake volumes actually corresponds to approximately 90% of the total volume of global fresh water lakes since the largest lakes (Baikal, Tanganyika, North American Great Lakes, Victoria) are well documented. For the remaining lakes lacking documented volume information, average lake depth was estimated as a function of lake area class (ESRI 1995) depending on glacial, non-glacial or tectonic origin (Meybeck 1995). Lake volume was calculated as the product of estimated lake depth and surface area. For the globe, we obtained a mean residence time in lakes of approximately 1.2 years.

All residence times are expressed in units of years. The calculations for τ represent theoretical hydraulic residence times and we recognize that they do not yield absolute residence times. τ for soil does not explicitly track nitrogen pathways in vegetation or soil organic matter. As we will see, it does, however, give a relative measure of leaching and potential nitrogen throughput that can be used to distinguish the transport behavior of individual drainage basins.

Basin-scale nitrogen flux model formulation

We developed independent statistical relationships linking present-day DIN and TN area-specific fluxes from GEMS/GLORI to the contemporary Nmob loadings and drainage basin attributes, based on non-linear least squares regression equations (JMP; SAS, Inc., Durham, NC) to yield estimates of riverine nitrogen flux (Nrf). Each equation was developed by exploring links between GEMS/GLORI specific yields (kg N km^2/year), basin-wide Nmob loads for actively flowing areas, and the additional drainage basin attributes listed in Table 1. The core of the Nrf flux equations resides in a set of nitrogen delivery coefficients (efficiencies E), which define the fraction of the total basin Nmob load that is delivered to the mouth. Delivery coefficients are represented as fractions between 0 and 1 of the Nmob mass transported through each of the following pathways: (a) soils and groundwater, (b) natural lakes, (c) reservoirs and (d) river networks.

Combining the delivery coefficients and Nmob loads the TN and DIN Nrf flux equations take the form:

$$\mathrm{Nrf} = E_{\mathrm{riv}} E_{\mathrm{res}} E_{\mathrm{lake}} (\mathrm{PtS} + \mathrm{NonPtS}_{\mathrm{org}}\, E_{\text{soil-org}} + \mathrm{NonPtS}_{\mathrm{inorg}}\, E_{\text{soil-inorg}}) \qquad (1)$$

where PtS is the specific point source loading, $\mathrm{NonPtS}_{\mathrm{org}}$ is the organic non-point source loading weighted by runoff, $\mathrm{NonPtS}_{\mathrm{inorg}}$ is the inorganic non-point source load weighted by runoff. The Nmob loadings were specifically assigned as follows:

$$\begin{aligned}
\mathrm{PtS} &= \text{Nmob load from sewered urban population} \\
\mathrm{NonPtS}_{\mathrm{org}} &= (\text{Nmob fixation} + \text{Nmob livestockload} \\
&\qquad + \text{Nmob NPS human load})(\text{runoff}/\text{precipitation}) \\
\mathrm{NonPtS}_{\mathrm{inorg}} &= (\text{Nmob deposition} + \text{Nmob fertilizer})(\text{runoff}/\text{precipitation}) \qquad (2)
\end{aligned}$$

where precipitation and runoff values are in mm/year and all Nmob loadings are in kg N km^2/year. Non-point source loads are weighted by available runoff to limit transport as a function of dryness. Non-point source loads were multiplied by the ratio of runoff to precipitation to represent an effective non-point source load to the land thereby weighting wetter basins with greater transport capacities than drier basins. Point sources as defined in this paper were not weighted by available water flow since they are assumed to be directly input into flowing river systems sufficient in size to transport the materials downstream. E_{riv}, E_{res}, E_{lake}, $E_{\text{soil-org}}$ and $E_{\text{soil-inorg}}$ are the delivery coefficients defining the fraction of incident Nmob

load transported through each system (river channels, reservoirs, lakes, and soils/groundwater, respectively). The non-point source loads were partitioned into organic and inorganic sources of Nmob to account for the different transformation processes associated with each. We recognize that some non-point source loads many contain a mixture of organic and inorganic forms, however we have chosen to assign each source load to their predominant component. The delivery coefficients take the form of:

$$E_{\text{riv}} = \mathrm{e}^{(-\tau_{\text{riv}} T_{\text{adj}} a_{\text{riv}})}, \qquad E_{\text{res}} = \mathrm{e}^{(-\tau_{\text{res}} T_{\text{adj}} a_{\text{res}})}, \qquad E_{\text{lake}} = \mathrm{e}^{(-\tau_{\text{lake}} T_{\text{adj}} a_{\text{lake}})},$$
$$E_{\text{soil-org}} = \mathrm{e}^{(-\tau_{\text{soil}} T_{\text{adj}} a_{\text{soil-org}})}, \qquad E_{\text{soil-inorg}} = \mathrm{e}^{(-\tau_{\text{soil}} T_{\text{adj}} a_{\text{soil-inorg}})} \tag{3}$$

where τ_{riv}, τ_{res}, τ_{lake}, and τ_{soil} are the specified residence times for river channels, reservoirs, lakes, and soils, respectively, T_{adj} (°C) is the average basin temperature normalized by adding 30 °C to eliminate the occurrence of negative values in the exponent, and the variables a_{riv}, a_{res}, a_{lake}, $a_{\text{soil-org}}$, and $a_{\text{soil-inorg}}$ are tunable parameters which define the shape of the respective constituent delivery functions. The delivery curves generally behave in an exponentially decreasing manner with increases in temperature and residence times. For example, with DIN we expect that higher temperatures will increase rates of denitrification and therefore decrease the delivery of Nmob downstream. Longer residence times increase the opportunity for nitrogen processing in the drainage basin landscape and aquatic systems *via* settling, uptake, and transformation and are also expected to decrease the delivery of DIN downstream. The tunable parameters were developed using a non-linear least squares regression analysis to find the best-fit values minimizing errors for the proposed model. We make estimates of TON by subtracting DIN from the TN estimates. Estimation algorithms for TN and DIN each converged in an objective function with a specified convergence criterion of 0.05. Coefficients and model performance measures for the TN and DIN nonlinear regression analysis are given in Table 2. Comparison of observed TN to the regression predicted values yielded a predicted/observed slope of 0.99 where the predicted TN values explained 88% of the variation in the observed TN values. The DIN regression predictions explained 68% of the variation in the observed DIN values and gave a predicted/observed slope of 0.94.TN and DIN fluxes for the pre-industrial state were generated using pre-industrial basin Nmob loadings and the resulting maps are thus fully simulated. Changes in climate were not considered for the pre-industrial state due to inaccuracies in currently available GCM's (National Assessment Synthesis Team 2001; Vörösmarty et al. 2000c) and their minor importance relative to the major forcings of the anthropogenic nitrogen loadings which increase considerably from pre-industrial to contemporary conditions. For the contemporary setting we made predictions for the more than 5 300 STN-30a basins. Our aim is to provide an accurate contemporary picture of loading. Thus, we 'burned-in' GEMS/GLORI observations of basin exports whenever available. Standard error estimates on mean annual fluxes were generated using JMP (SAS, Inc., Durham, NC). Statistical summaries for the globe, individual continents, and ocean basins were prepared.

Table 2. Non-linear least squares regression equation results and parameters.

Parameter	Estimate	ApproxStdErr	Lower CL	Upper CL
TN non-linear regression equation[a]				
a_{riv}	0.0858618033	0.04779342	−0.0178481	0.23250514
a_{res}	0.050900997	0.01298088	0.02593498	0.092499
$a_{soil\text{-}org}$	0.000164579	0	−0.0041304	0.0017604
$a_{soil\text{-}inorg}$	0.0149043286	0.00423667	0.00680154	0.04067316
a_{lake}	0.0004263108	0.00042079	−0.0001996	0.00408298
$Nrf_{TN} = E_{riv}E_{res}E_{lake}(PtS + NonPtS_{org}E_{soil\text{-}org} + NonPtS_{inorg}E_{soil\text{-}inorg})$				
DIN non-linear regression equation[b]				
a_{riv}	0.398674261	0.08455365	0.21962927	0.55705911
a_{res}	0.0337858888	0.01851732	0.0060824	–
$a_{soil\text{-}org}$	0.1104082556	0.04051463	0.06355603	–
$a_{soil\text{-}inorg}$	0.0011524393	0.00140753	−0.0007241	0.00503864
a_{lake}	0.0100626882	0.00250364	0.00572282	0.01538738
$Nrf_{DIN} = E_{riv}E_{res}E_{lake}(PtS + NonPtS_{org}E_{soil\text{-}org} + NonPtS_{inorg}E_{soil\text{-}inorg})$				
TON equation				
$Nrf_{TON} = Nrf_{TN} - Nrf_{DIN}$				

[a]Number of rivers = 58; variation explained by predicted TN = $1 - [\text{sum}(x-y)^2/\text{sum}(y-y_{mean})^2] = 0.88$; slope = 0.99; SSE = 1273456; DFE = 54; MSE = 23582; RMSE = 153.
[b]Number of rivers = 281; variation explained by predicted DIN = $1 - [\text{sum}(x-y)^2/\text{sum}(y-y_{mean})^2] = 0.68$; slope = 0.94; SSE = 2099561; DFE = 121; MSE = 17351; RMSE = 131.

Seasonal basin-scale nitrogen fluxes

Finally, we produce global, time-varying inputs of TN to the world's coastal zone, simulating a seasonal climatology of Nrf riverine flux. Monthly estimates of Nrf flux were derived as a function of the intra-annual variability in monthly water discharge acting as the predominant mechanism for transporting Nmob through the river system. Previous global studies have emphasized the correlation between runoff and Nrf export (Caraco and Cole 1999) and more current regional studies have illustrated the importance of hydrologic control over seasonal or intra-annual changes in leaching and export of Nrf at river mouths (Donner et al. 2002). For this analysis a monthly climatology of runoff (Fekete et al. 1999) was used to apportion the annual Nrf river flux according to simulated monthly discharge fields. Each month was assigned a percentage of the annual Nrf flux according to the amount of annual discharge represented in that month. The Nrf monthly river fluxes were summarized into four seasons.

A preliminary analysis of the discharge-apportioned Nrf river flux was carried out for rivers in the USGS National Stream Water Quality Monitoring Networks (WQN) database (Alexander et al. 1995) using monthly average discharge from daily observations and daily nitrogen concentrations to produce monthly and sea-

sonal estimates of DIN flux. The WQN database was comprised of 679 rivers spanning the US covering 33 years of daily monitoring observations from 1962 through 1995. Basins ranged in size from 10 000 km^2 to 3×10^6 km^2. This analysis showed that 76% of the observed seasonal DIN flux was accounted for by using the monthly discharge-apportioned method. Based on these results we consider the Nrf seasonal river flux model presented here adequate to represent a sufficient portion of the intra-annual variability in nitrogen flux at river outlets.

Results: a geography of global Nmob loading and Nrf basin flux

The maps and figures in this section summarize results for the loading of reactive Nr onto the landmass, the resulting local nitrogen loads mobilizable to inland aquatic systems (Nmob), the transport through inland waters, and eventual delivery to receiving waters. Data is presented for both the pre-industrial and contemporary states at grid cell and basin scale resolutions for TN, DIN, and TON. An estimate of the percent change in nitrogen loading and flux from pre-industrial to the contemporary time frame is given, as is a geography of the overall efficiency of transport. The key determinants of nitrogen loads across the landmass are identified to help understand the role of present-day anthropogenic loading on the global nitrogen cycle. We also present seasonal fluxes of TN for the globe.

Nmob loading to the continental landmass

Mobilizable nitrogen loading for the pre-industrial and contemporary landmass is shown in Figure 2. For the pre-industrial state, the largest amounts of Nmob loads are seen in the tropics, a reflection of substantial amounts of Nr fixation (Figure 3(A)). Large increases in the amount of Nmob loaded to the landmass are seen in the contemporary state with the greatest increases occurring in the temperate and sub-tropical zones. In the pre-industrial state Nmob loading does not exceed 2 MT Nr km^{-2}/year whereas in the contemporary state values in excess of 5 MT Nr km^{-2}/year are common. Largest contemporary loads are seen in central and eastern North America, throughout Europe, and in southern and southeastern Asia. There are increases in Nmob loading in tropical areas in the contemporary relative to the pre-industrial state but for the most part the ranges are similar.

Distribution of the Nmob loads relative to the Köppen climate zone classification system is illustrated in Figure 3(A). The horizontal lines superimposed on the contemporary loading bars represent the level of uncorrected Nr atmospheric loading of contemporary deposition and fixation. Under contemporary conditions the uncorrected Nr fixation and deposition levels show an increase for all climate classes relative to the pre-industrial state. However, the mass balance corrected Nmob fixation and deposition levels, shown as yellow bars, are similar to the pre-industrial with minor net gains in the cold and temperate zones and a slight net

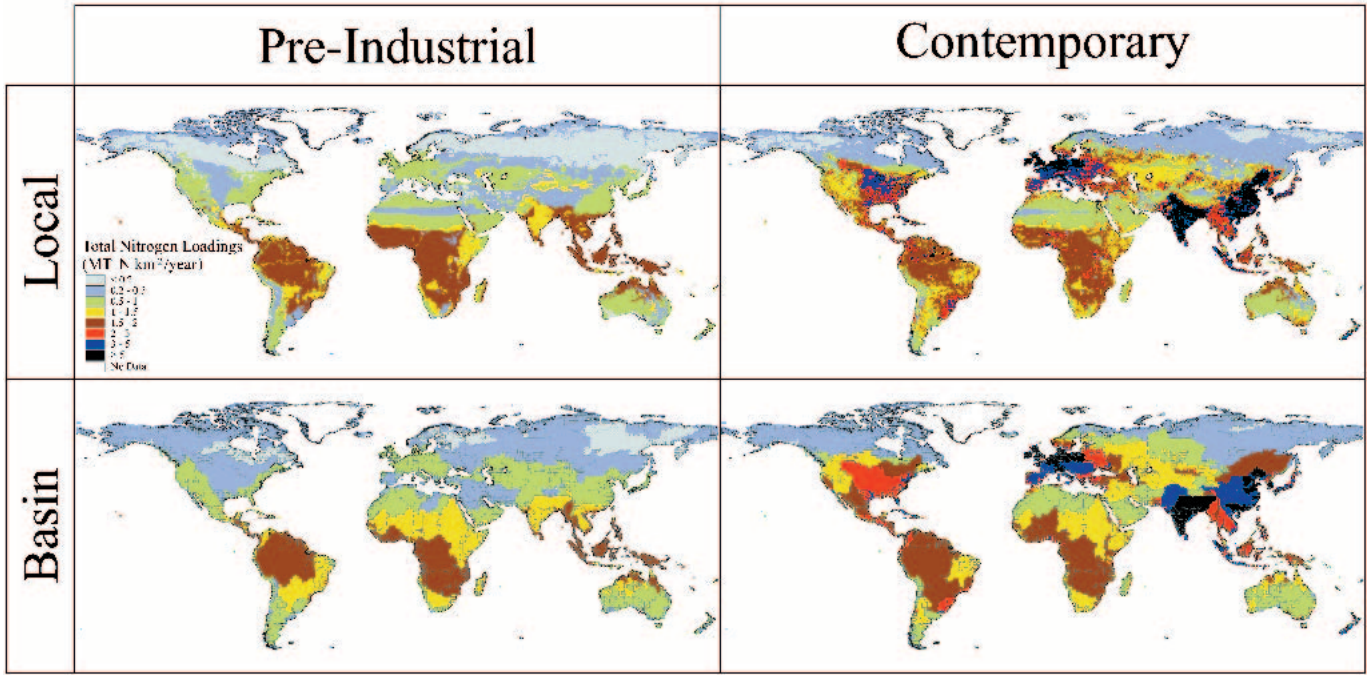

Figure 2. Pre-industrial and contemporary (mid-1990s) distribution of specific Nmob loading onto the continental landmass (kg N km^{-2}/year). Upper panel: 30′ (longitude × latitude) resolution mapping ($n = 59\,132$ grid cells). Lower panel: basin-sale loads ($n = 6\,152$ potentially discharging basins; Vörösmarty et al. 2000).

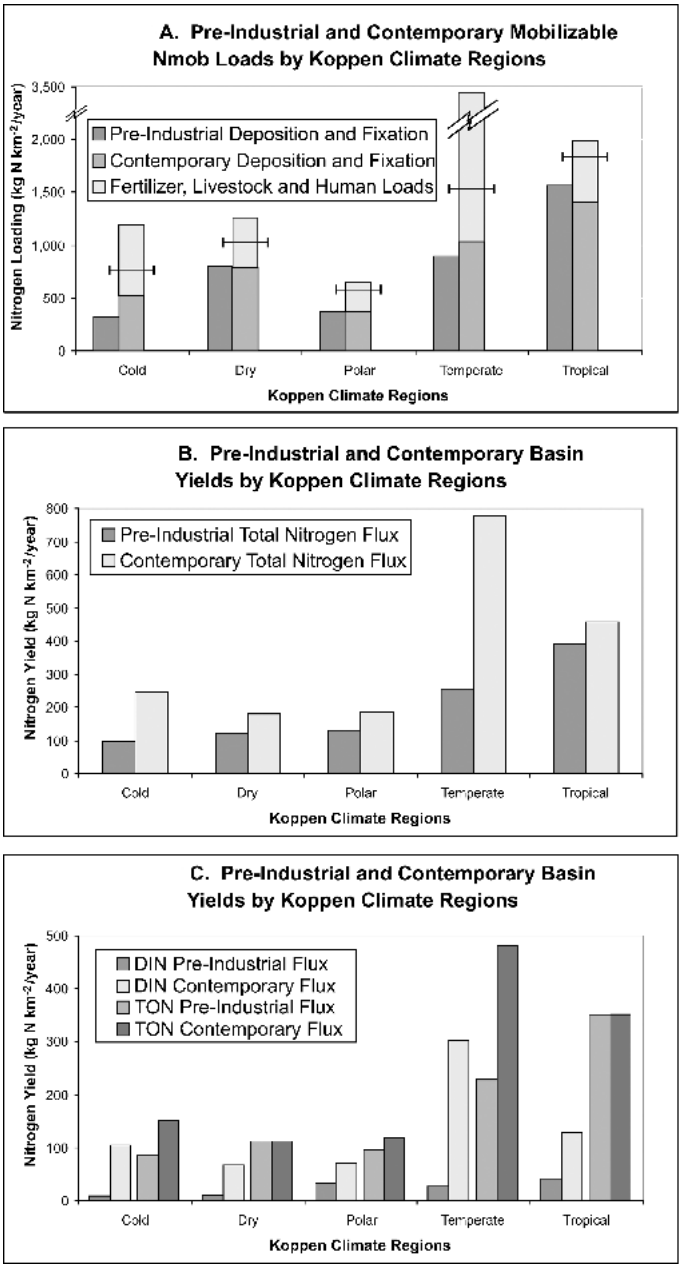

Figure 3. Pre-industrial and contemporary (mid-1990s) distribution of (a) specific Nmob loads (kg N km^{-2}/year), (b) total Nr river yields (kg N km^{-2}/year), and (c) DIN and TON river yields (kg N km^{-2}/year), for different climate zones. The horizontal lines superimposed on the contemporary loading bars in (a) represent the level of uncorrected Nr atmospheric loading of contemporary deposition and fixation.

Table 3. Pre-industrial and contemporary mobilizable nitrogen loading.

	Pre-industrial Nmob			Contemporary Nmob					
	Deposition (Tg/year)	Fixation (Tg/year)	Total (Tg/year)	Deposition (Tg/year)	Fixation (Tg/year)	Fertilizer (Tg/year)	Livestock load (Tg/year)	People load (Tg/year)	Total (Tg/year)
(A) Continent									
Africa	3.63	31.99	35.61	6.58	25.02	0.94	6.43	2.25	41.22
Asia	3.29	25.45	28.73	11.21	22.62	20.21	22.41	12.70	89.15
Australia	0.46	6.99	7.45	0.46	5.70	0.19	1.48	0.09	7.91
Europe	0.62	3.92	4.54	4.40	3.06	5.48	10.13	3.09	26.16
North America	1.27	9.81	11.07	6.16	8.76	5.48	5.85	1.95	28.21
Oceania	0.02	0.34	0.35	0.03	0.17	0.07	0.58	0.02	0.87
South America	2.75	20.16	22.91	3.51	16.12	1.59	6.63	1.21	29.06
(B) Ocean basin									
Arctic Subocean	0.61	3.41	4.02	2.11	3.26	0.24	0.90	0.31	6.83
Atlantic Ocean	5.65	41.62	47.27	13.68	34.47	10.31	17.69	4.79	80.94
Black Sea	0.16	1.07	1.24	1.01	0.79	0.83	3.19	0.89	6.72
Indian Ocean	1.96	20.03	21.99	4.80	16.36	6.28	13.64	5.26	46.34
Land	1.12	11.82	12.94	3.37	10.12	0.96	4.50	1.56	20.52
Mediterranean Sea	0.62	5.83	6.45	1.90	4.45	1.56	2.91	1.33	12.15
Pacific Ocean	1.91	14.89	16.80	5.48	12.01	13.78	10.67	7.18	49.11
Global totals	12	99	111	32	81	34	54	21	223
Original atmospheric Nr sources				44	112*	71**			

*Fixation corrected for Nr loss due to biomass burning and natural soils emissions.

**Fertilizer corrected for Nr loss due to NH_3 volatilization.

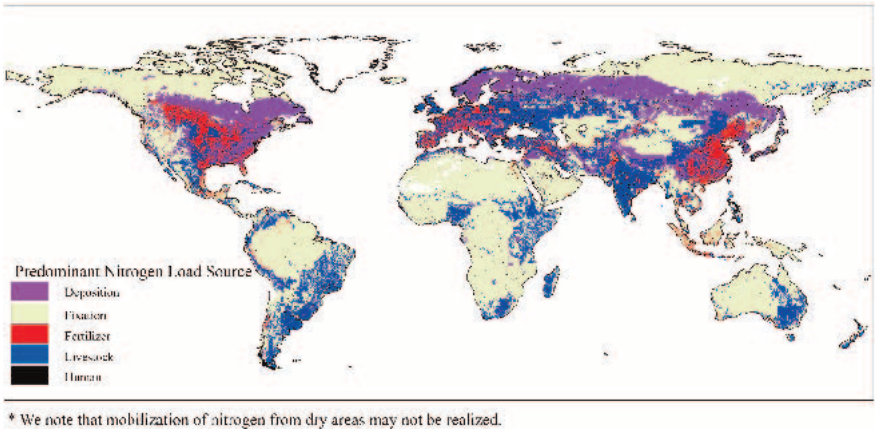

Figure 4. Predominant source of Nmob loading under the contemporary setting. Categories represent one of the five contemporary nitrogen sources (deposition, fixation, fertilizer, livestock, and human loads) based on total Nmob load to the grid cell.

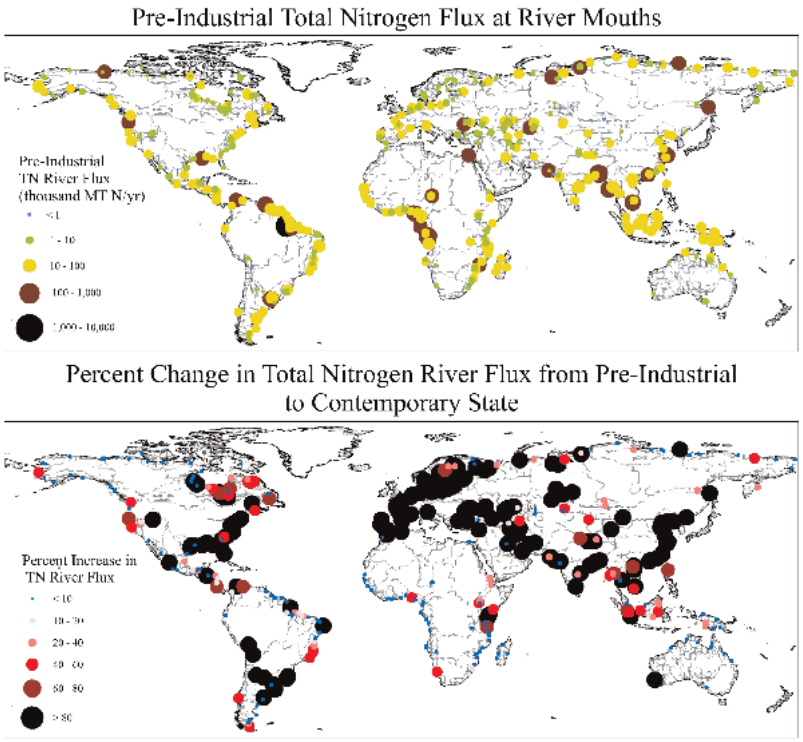

Figure 5. Fluvial TN fluxes, showing pre-industrial mouth-of-river fluxes and the relative change for contemporary conditions ($n = 387$ actively discharging basins $<25\,000\,\mathrm{km}^2$).

decrease in the tropical zone. Additional anthropogenic contemporary loads in the form of fertilizer, livestock and human emissions (red bars) are substantial in each climate zone. In relative terms they are largest for cold and temperate climates. The largest relative and absolute increase has occurred in the temperate zone.

Table 3(A) and (B) shows global, continental, and coastline-specific estimates of mobilizable nitrogen loadings onto the continental landmass, contrasting pre-industrial and contemporary conditions. Nmob loading to the landmass for the pre-industrial state is 111 Tg/year. Pre-Industrial deposition and fixation global estimates are similar to previously reported estimates (Dentener and Crutzen 1994; Smil 1999) and are lower but still consistent with those recently reported by Galloway et al. (2003) (Galloway estimates 17 Tg/year deposition and 125 Tg/year fixation). In the contemporary state the Nmob loading is increased to 223 Tg/year due to the introduction of additional anthropogenic sources, from industrial deposition, managed crop associated fixation and industrial fertilizers. Global totals for the original contemporary net atmospheric Nr sources are provided at the bottom of Table 3 for comparison to the redistributed contemporary Nmob loads. The undistributed contemporary net atmospheric Nr deposition, fixation, and fertilizer global totals are all similar to previously reported estimates (Dentener and Crutzen 1994; Smil 1999; Seitzinger et al. 2002a) and lower but still consistent with those recently reported by Galloway et al. (2003) (Galloway estimates 63 Tg/year deposition, $\sim$139 Tg/year natural + cultivated fixation, and 100 Tg/year industrial fertilizer with 86 Tg/year accounting for process losses).

In the pre-industrial state the single largest contributor of Nmob to the landscape is fixation, which holds across all continents and receiving ocean basins. For the contemporary state the largest Nmob contributors continue to be fixation followed by livestock, fertilizer, deposition and human loading, in that order. Asia and the Atlantic Ocean river basins receive the greatest total amount of Nmob loading to the landscape (89 and 81 Tg/year, respectively) while Oceania and the Black Sea basins show the lowest total loading of Nmob (0.87 and 6.72 Tg/year, respectively). The European continent and the Black Sea drainage basins receive the greatest Nmob load per contributing basin area (3 043 and 3 296 kg N km^{-2}/year, respectively) while North America and the Arctic Subocean river basins have the lowest loading of Nmob per basin area (1 756 and 640 kg N km^{-2}/year, respectively).

Figure 4 represents the contemporary distribution of Nmob loads to the landmass mapped by the predominant contributor of nitrogen within each 30′ grid cell. It can be seen that fixation is the primary source of Nmob load throughout South America, Africa, Australia, and the northernmost reaches of Asia and North America. Deposition plays a dominant role throughout the northern temperate zones of Europe, Asia and North America. Fertilizer Nmob load is predominant in the agricultural areas of the world including, the 'bread basket' of the US and Canada, throughout continental Europe, and eastern China. Livestock loading is the most important Nmob source in Eastern Europe and India and plays an important role in South America, Africa, and Australia. Human Nmob loadings can be seen as single grid

Table 4. Pre-industrial and contemporary nitrogen fluxes.

	Pre-industrial				Contemporary			
	Total Nmob loads (Tg/year)	Total N flux (Tg/year)	Transport efficiency (%)	Total Nmob loads (Tg/year)	Total N flux (Tg/year)	Transport efficiency (%)	Median τ (years)	Mean temperature (°C)
(A) Continent								
Africa	35.61	3.14	9	41.22	2.42	6	1.38	23.1
Asia	28.73	7.39	26	89.15	18.71	21	0.82	8.5
Australia	7.45	0.29	4	7.91	0.33	4	2.22	19.9
Europe	4.54	1.17	26	26.16	6.19	24	1.13	4.9
North America	11.07	2.63	24	28.21	4.53	16	1.47	−3.4
Oceania	0.35	0.18	51	0.87	0.37	42	0.60	15.5
South America	22.91	6.24	27	29.06	7.51	26	0.65	17.1
(B) Ocean basin								
Arctic Ocean	4.02	1.30	32	6.83	2.64	39	1.50	−11.6
Atlantic Ocean	47.27	9.77	21	80.94	15.10	19	1.18	11.4
Indian Ocean	21.99	3.23	15	46.34	7.43	16	1.02	23.5
Land	12.94	0.89	7	20.52	1.43	7	6.72	7.4
Mediterranean + Black Sea	7.69	0.58	8	18.87	2.25	12	1.65	12.9
Pacific Ocean	16.80	5.30	32	49.11	11.23	23	0.63	13.3
Global totals	111	21	19	223	40	18	1.13	6.1

cell localized 'hotspots' primarily associated with large urban settlements (i.e., New York City, USA; Mexico City, Mexico; Sao Paolo, Brazil; London, UK, etc.).

Nitrogen flux at river mouths

Figure 5 shows the spatial distribution of riverine nitrogen fluxes for the globe. The figure compares pre-industrial Nrf fluxes at river mouths and the percent change from the pre-industrial to the contemporary state. The largest pre-industrial Nrf riverine fluxes are associated with the biggest rivers where the Amazon has the largest Nrf flux exceeding 3.3 million MT N/year. In the contemporary state the largest increases in Nrf riverine flux are evident in the industrialized world of North America and continental Europe as well as southern and southeast Asia. As seen in Figure 2 these areas also receive the largest increase in contemporary Nmob loads to the landmass and aquatic systems. There are relative increases in Nrf riverine flux in some tropical rivers for the contemporary state, particularly in South America, however they are not as evident as the temperate zone impacts.

Table 4(A) and (B) presents global, continental, and ocean basin estimates of riverine fluxes for TN from the continental landmass, contrasting pre-industrial and contemporary conditions. Median residence times (Tau) and mean annual temperatures are provided for basins organized by continent and receiving ocean basin. TN flux for the pre-industrial state is 21 Tg/year representing a 19% transport efficiency of nitrogen from land to river outlet. In the contemporary state the TN flux increases to 40 Tg/year but overall transport efficiency is virtually identical (18%). These values are similar to previously reported estimates of Nrf riverine flux ($\sim$44 Tg/year TN from Seitzinger et al. 2002a) and transport efficiencies ($\sim$20% from Howarth 1998; Seitzinger et al. 2002a) and are lower but still consistent with the 25% transport efficiency estimate recently reported by Galloway et al. (2003) for the globe and Howarth et al. (2002) and Boyer et al. (2002) for the northeastern US. Each of the continents shows slight to moderate decreases in their contemporary efficiencies relative to pre-industrial. The largest emitter of total riverine nitrogen is Asia (19 Tg/year) while the lowest is Australia (0.3 Tg/year). The largest continental yields of total riverine Nrf flux are in Oceania (895 kg N km^{-2}/year) whereas the lowest are in Australia (43 kg N km^{-2}/year). The continents with the lowest transport efficiencies are Africa and Australia, which are also the driest continents. Both continents have very high mean annual temperatures coupled with high (Australia) to moderate (Africa) residence times suggesting an enhanced capacity to process nitrogen in basin resulting in less Nrf flux delivered to the river mouth. The highest efficiency of transport is associated with Oceania, a region characterized by small rivers with low residence times suggesting a diminished capacity to process nitrogen in basin and therefore a greater throughput of nitrogen to river mouth. Next highest is South America, which also has low residence times reflecting lower nitrogen processing capabilities. In both these cases, the shorter residence times may predominate over the potential metabolic effects of moderate to high mean temperatures in these basins yielding greater transport efficiencies.

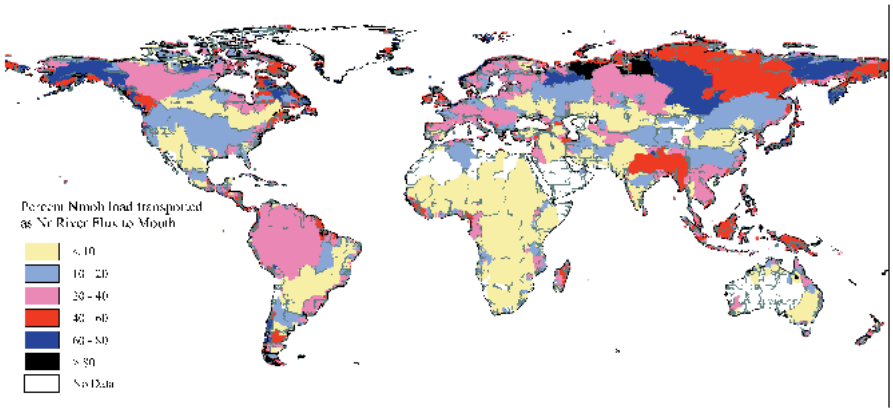

Figure 6. Total N transport efficiencies for drainage basins ($n = 387$ actively discharging basins $>25\,000\,\mathrm{km}^2$). Mean transport is 18% globally, with a range from 0 to 100%. The range and geography can be explained by variations in temperature and residence time (see Eq. (1)).

In the pre-industrial state the Arctic and Pacific Ocean basins show the highest transport efficiencies for TN. In the contemporary state the Arctic Ocean draining basins show by far the largest transport efficiency. We hypothesize that the Arctic basins are characterized by very low temperatures which limit biological nitrogen processing within basin and therefore support greater throughput of Nrf flux to river mouth. In some areas we see a sensitivity to anthropogenic loads related to the product of residence time and temperature. The transport efficiency for the Pacific Ocean draining basins decreases from 32% pre-industrial to 23% for the contemporary state. Moderate to high mean annual temperatures in many of these basins may support a greater biological processing capacity and hence reduce the amount of additional contemporary Nmob loading reaching the ocean as Nrf flux. The lowest transport efficiencies are associated with the endorheic (Land) basins which exhibit very high residence times providing a greater time period over which to process loaded nitrogen in basin hence reducing the amount reaching river mouth as Nrf flux.

Figure 6 shows the contemporary spatial distribution of Nmob transport efficiency. Transport efficiencies range from 0 to 100% with a global mean of 18%. The largest efficiencies are evident in the colder regions of the globe with efficiencies exceeding 60% for many of the Arctic draining rivers. As seen in Table 4 these high efficiencies arise from low temperatures which reduce the capacity for biotic processing of the transported Nmob. Typically, the tropics have lower transport efficiencies seldom exceeding 20% attesting to their ability to optimally process Nmob within most basins despite high hydraulic throughput. However, there are some rivers in Africa, South America, and most notably, over much of Indonesia which have efficiencies exceeding 40%. These higher efficiencies arise in relatively smaller basins, typically mountainous areas with very high runoff, resulting in very short residence times and reduced opportunities for processing of Nmob. Some of the lowest transport efficiencies are seen for rivers with altered flow

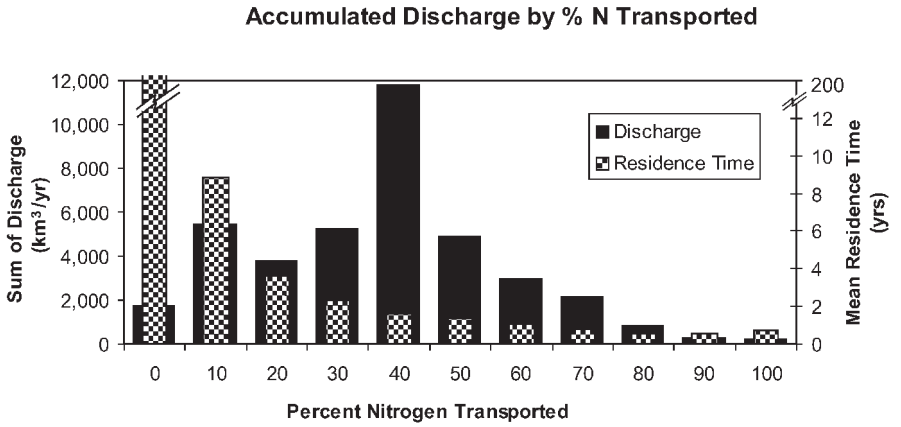

Figure 7. Accumulated discharge (km^3/year) and residence time (years) grouped by Nr transport efficiency class (Nrf flux at river mouth/Nmob load in river basin).

receiving little to no discharge at river mouth such as the Colorado, Rio Grande, Nile, Indus and Amu-Darya.

Distribution of the nitrogen riverine specific yields, aggregate transport, and transport efficiency with respect to the Köppen climate zone classification system is illustrated in Figure 3(B) for TN. Similar to the Nmob loading from Figure 3(A) the largest Nrf riverine fluxes from the landmass in the pre-industrial state occur in the tropical zone in Figure 3(B). For the contemporary state Nrf fluxes in the tropical, polar and dry zones increase only slightly. More pronounced increases are seen in the cold and temperate zones. Nrf riverine fluxes in the temperate zone dominate the contemporary state, mirroring the excess anthropogenic loads seen in Figure 3(A) for the temperate zone.

Figure 3(C) shows Nrf riverine fluxes by Köppen climate zone classification system for DIN and TON. The general trend of DIN and TON river fluxes across climate zones generally follows that seen in Figure 3(B) for TN. DIN river fluxes show large increases from the pre-industrial to contemporary state in all classes with the greatest increases evident in the temperate and cold zones. TON fluxes show little change from pre-industrial to contemporary for the dry and tropical zones and minor to moderate increases in the polar and cold zones, respectively. The greatest increases in TON river flux are seen in the temperate zone where TON fluxes show a near doubling from pre-industrial conditions. This increase in TON flux is consistent with the very large increases in contemporary TN and DIN fluxes evident for the temperate zone (Figure 3(B) and (C)). Globally, DIN river fluxes are highest in the temperate zone while TON river fluxes play a dominant role in both the temperate and tropical zones.

Figure 7 shows the cumulative frequency histogram of accumulated discharge and residence times in basins occurring in 10% transport efficiency groupings. This figure demonstrates the majority of the discharge occurs in basins transporting 40%

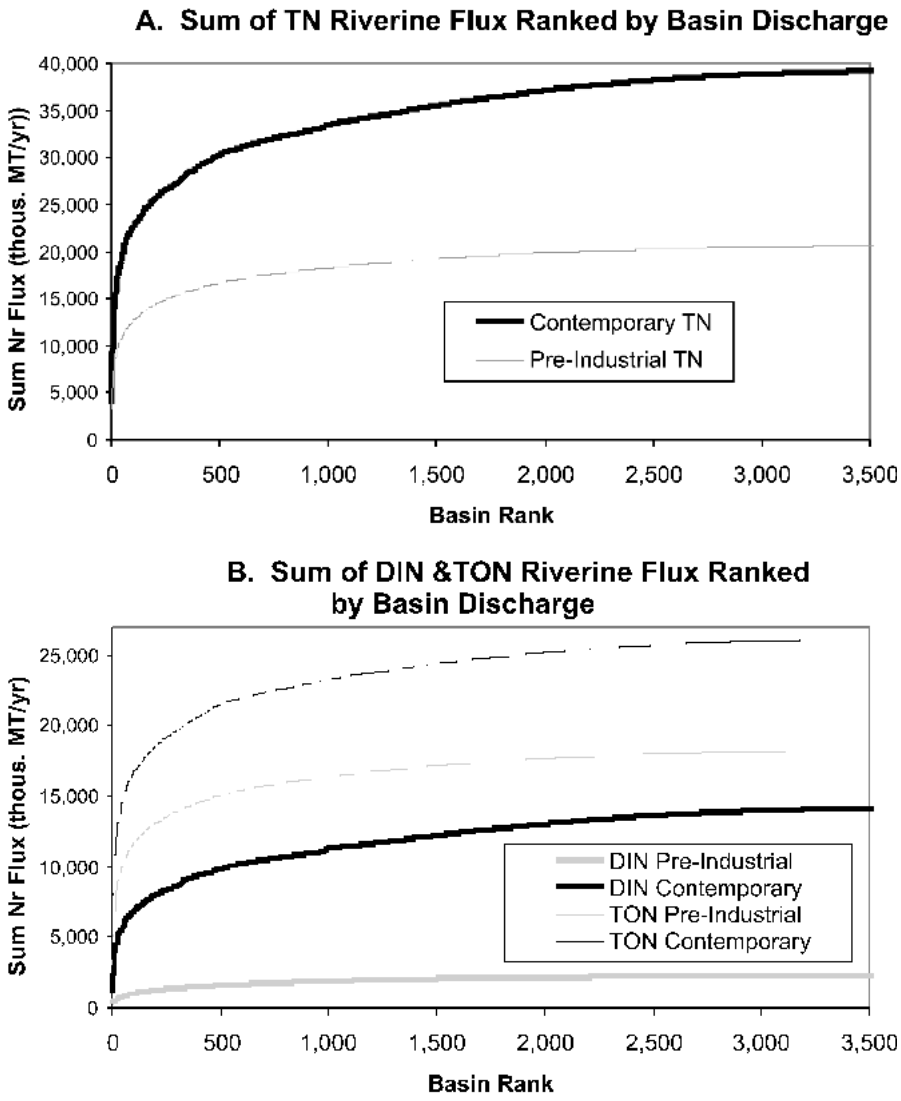

Figure 8. Pre-industrial and contemporary (mid-1990s) cumulative riverine flux for (a) TN and (b) DIN and TON ranked by basin discharge. Basins were ranked from largest to smallest discharge starting with the Amazon at rank = 1.

Nrf or less. Very little discharge is associated with efficiencies exceeding 70%. Although both temperature and residence time control overall efficiency of transport, a clear inverse relationship is apparent between computed transport efficiencies and basin residence times. Comparison of transport efficiencies with basin residence times shows basins with higher residence times exhibit lower transport efficiencies; as mean residence times decrease transport efficiencies increase.

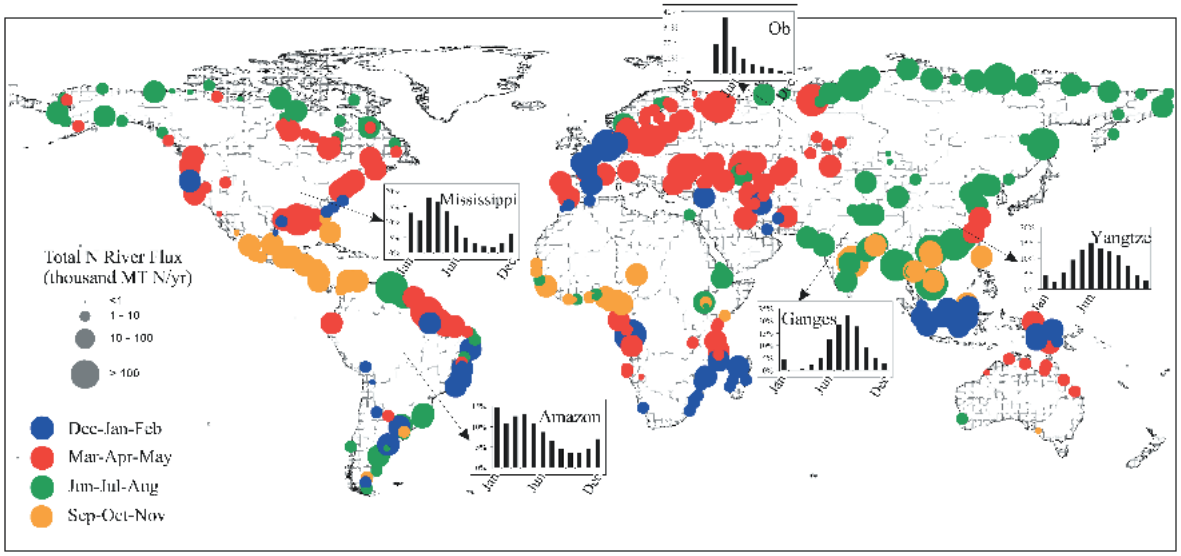

Figure 9. Seasonal distribution of Nrf riverine flux at basin mouths represented by colored disks illustrating the magnitude of Nrf flux and time period of maximum discharge. The color of the disk corresponds to the monthly time period shown in the legend; the size of the disk relates to the total amount of Nrf flux discharging from the river in the prescribed seasonal time block ($n = 387$ actively discharging basins $>25\,000\,\mathrm{km}^2$).

Figure 8(A) and (B) shows saturating curves for the accumulated TN, DIN and TON fluxes for pre-industrial and contemporary conditions as a function of basin ranked by descending water discharge. In all cases the contemporary Nrf flux for TN, DIN and TON quickly exceeds the Pre-Industrial Nrf river flux and asymptotes after approximately the 3 000 highest discharging basins. Total accumulated contemporary Nrf river flux is nearly twice as large as the pre-industrial flux for TN. Pre-industrial DIN river flux is low compared to TON flux, however, these fluxes increase by 3-fold in the contemporary condition. Pre-industrial TON river fluxes comprise the bulk of the total Nrf fluxes and continue to increase 1.5 times in the contemporary state.

Seasonal transport of nitrogen

Figure 9 shows the seasonal distribution of Nrf riverine flux at basin mouths for the globe. The Nrf riverine flux is represented by colored disked illustrating the magnitude of Nrf flux and time period of maximum discharge. The color of the disk corresponds to the monthly time period shown in the legend; the size of the disk relates to the total amount of Nrf flux discharging from the river in the prescribed monthly time block (larger disks = larger fluxes).

Temperate zone rivers generally peak in the March through May monthly period reflecting a spring thaw flux of nitrogen in rivers for this region. The Nrf flux wave is delayed in the northern temperate and polar zones reaching its peak in the June through August time period corresponding with a later snowmelt. Rivers in the tropical regions typically exhibit a longer peak discharging period and peak in the December through May time period for the equatorial regions of South America, Africa, Indonesia and Northern Australia. Sub-tropical rivers farther north of the equator in Central America and the Sahel region of Africa exhibit later peaks beginning in June and lasting through November. Much of Asia sees peak Nrf fluxes from March through August with the monsoon influenced regions of southern Asia peaking in June through August.

From a regional coastline perspective, land-to-ocean fluxes in many areas occur as sequential pulses of Nrf delivery (e.g., red/green mixes in east Asia, blue/red mixes in equatorial Africa and South America). This represents the impact of differential runoff source areas and travel time variations (Vörösmarty et al. 2000). This in turn represents the spatial distribution of Nmob loads within these different sized basins and the time required to move the bulk of these loads through the basin to the river mouth. Thus, while in aggregate more Nmob may be loaded onto large basins ($>500\,000\,km^2$), small basins ($<100\,000\,km^2$) are typically more effective at transporting those loads that they receive and maintain a relatively shorter flux period. For example, in eastern China all large basins show Nmob = 18 Tg/year and Nrf riverine flux = 3 Tg/year whereas all small basins have Nmob = 4 Tg/year and Nrf riverine flux = 5 Tg/year. Thus, for the entire coastline of eastern China, we see 17% transport for large basins and 37% transport for small basins, with an overall average of 23% transport efficiency for the entire coastline. In addition, due to shorter travel times, smaller basins show Nrf riverine flux peaks occurring earlier in

the season (March through May for smaller basins in eastern China) coincident with peak precipitation where larger basins in the same region can exhibit a temporal delay in peak fluxes (June through August for larger basins in this same region).

Summary and conclusions

A model of nitrogen export to the coastal zone requires a comprehensive knowledge of the spatial distribution and magnitude of Nr sources loaded to the land and aquatic systems coupled with an understanding of the processes for removal and transformation of this Nr as it moves through various systems along its journey to the river mouth. A basin explicit, empirical modeling approach is used here developed from subsidiary input loading at a much finer gridded resolution to estimate TN, DIN and TON export to coastal systems for the globe. The statistical Nrf riverine flux model utilizes a set of transport coefficients to move mobilizable source nitrogen loads through the land and aquatic systems accounting for Nr losses due to transformations and sinks. The results of the Nrf riverine flux model indicate that large increases in anthropogenic loads of nitrogen to the landmass and aquatic systems influence fluxes of both TN and DIN at river mouths for the global and regional–continental scales. An analogous paradigm is also reflected in the TON flux estimates which are a product of the model estimated TN and DIN fluxes. The impacts of increased loading in the industrialized world in the contemporary era are clearly evident in the subsequent increases in riverine Nrf flux at basin mouths. Model results also demonstrate the spatial heterogeneity of changes in loading and responses to load increases throughout the world. Variations in transport capacities for different parts of the world suggest that certain areas of the globe are more sensitive to increasing loads where other areas are better able to process excess loads within basin and hence mitigate increasing fluxes at river mouth.

Although the current model addresses nitrogen processes and transformations within the river basin in a *lumped* fashion, we do not claim to provide an exhaustive accounting of the individual processes on a spatially distributed level. A greater understanding of the sequestration and storage of nitrogen in regrowing systems as well as the spatially explicit nature of denitrification across the landscape and within aquatic systems is needed, neither of which is expressly addressed in the current model. We are also limited by the non-specificity of currently available global crop assignment data sets. In addition, seasonal aspects of land based and aquatic processes and activities including seasonal cropping and fertilizer application as well as variations in natural and crop fixation throughout the year require further analysis.

Central to a comprehensive understanding of the dynamics of nitrogen transport in river systems is the increased availability of monitoring data which is not uniformly available for all parts of the global. An increase in the availability of in-stream measurements at river mouths and along reaches for constituents will greatly facilitate future modeling initiatives by providing a known baseline for calibration and comparison of model results. Lack of observed data is expressly crucial for the

developing world where a limited amount of information is currently available. Of particular importance is the availability of monitoring data for intra-annual time series and/or climatologies to enhance our understanding and modeling of seasonal variations of nutrients throughout the world. The current analysis is an important first step towards modeling of monthly and seasonal nitrogen fluxes to the coastal zone at the global scale.

Acknowledgements

This work was supported by funding (to UNH) from NASA SeaWIFS Project (NAG5-10260, NAG5-12451), Office of Naval Research (ONR) (N00014-01-1-0357), and NASA Interdisciplinary Science (IDS) (NAG5-10135). This work was initially spearheaded as a part of the International SCOPE Nitrogen Project, which received support from both the Mellon Foundation and from the National Center for Ecological Analysis and Synthesis (NCEAS) in Santa Barbara, California. Special thanks to Joe Salisbury, Janet Campbell, Dave Meeker, Mark Dowell, Bill McDowell, Ernst Linder, Balazs Fekete, Richard Lammers and Bob Howarth for useful discussion during the development of this project and Stanley Glidden for his continued support. We appreciate the input of the two anonymous reviewers and recognize their contribution to the publication of this paper.

References

Alexander R.B., Slack J.R., Ludtke A.S., Fitzgerald K.K. and Schertz T.L. 1995. US Geological Survey National Stream Water-Quality Monitoring Networks (WQN), USGS Digital Data Series DDS-37.

Alexander R.B., Smith R.A. and Schwarz G.E. 2000. Effect of stream channel size on the delivery of nitrogen to the Gulf of Mexico. Nature 403(6771): 758–761.

Billen G. and Garnier J. 1999. Nitrogen transfers through the Seine drainage network: a budget based on the application of the 'Riverstrahler' model. Hydrobiologia 410: 139–150.

Bouwman A.F. and Boumans L.J.M. 2002. Estimation of Global NH_3 volatilization loss from synthetic fertilizers and animal manure to arable lands and grasslands. Biogeochem. Cy. (in press).

Bouwman A.F., Lee D.S., Asman W.A.H., Dentener F.J., Van Der Hoek K.W. and Olivier J.G.J. 1997. A Global High-Resolution Emission Inventory for Ammonia. Global Biogeochemical Cycles 11(4): 561–587.

Boyer E.W., Goodale C.L., Jaworsk N.A. and Howarth R.W. 2002. Anthropogenic nitrogen sources and relationships to riverine nitrogen export in the northeastern USA. Biogeochemistry 57(1): 137–169.

Caraco N. and Cole J. 1999. Human impact on nitrate export: an analysis using major world rivers. Ambio 28: 167–170.

Cleveland C.C., Townsend A.R., Schimel D.S., Fisher H., Howarth R.W., Hedin L.O., Perakis S.S., Latty E.F., Von Fischer J.C., Elseroad A. and Wasson M.F. 1999. Global patterns of terrestrial biological nitrogen (N_2) fixation in natural systems. Global Biogeochem. Cy. 13: 623–645.

Covich A.P. 1993. Water and ecosystems. In: Gleick P.H. (ed) Water in Crisis: A Guide to the World's Fresh Water Resources. Oxford University Press, Oxford, pp. 40–55.

Dentener F.J. and Crutzen P.J. 1994. A three dimensional model of the global ammonia cycle. J. Atmos. Chem. 19: 331–369.

Donner S.D., Coe M.T., Lenters J.D., Twine T.E. and Foley J.A. 2002. Modeling the impact of hydrological changes on nitrate transport in the Mississippi River Basin from 1955 to 1994. Global Biogeochem. Cy. 16(3): 1043.

Elvidge C.D., Baugh K.E., Kihn E.A., Kroehl H.W. and Davis E.R. 1997. Mapping city lights with nighttime data from the DMSP operational linescan system. Photogrammetric Eng. Remote Sensing 63(6): 727–734.

(EDC) Earth Resources Observation Systems (EROS) Data Center 2000. Global Land Cover Characterization. EROS Data Center Distributed Active Archive Center. http://edcdaac.usgs.gov/.

Environmental Systems Research Institute, Inc. (ESRI) 1995. Arc World Supplement, 1:3 M scale digital map. Environmental Systems Research Institute, Inc., Redlands, CA.

Food and Agriculture Organization of the United Nations (FAO) 2001. FAOSTAT: FAO Statistical Databases. Accessible through the Food and Agriculture Organization of the United Nations. http://apps.fao.org/.

Fekete B.M., Vörösmarty C.J. and Grabs W. 1999. Global, Composite Runoff Fields Based on Observed River Discharge and Simulated Water Balances. WMO-Global Runoff Data Center Report #22. Koblenz, Germany.

Fekete B.M., Vorosmarty C.J. and Grabs W. 2002. High-resolution fields of global runoff combining observed river discharge and simulated water balances. Global Biogeochem. Cy. 16(3): 1042.

Galloway J.N., Dentener F.J., Capone D.G., Boyer E.W., Howarth R.W., Seitzinger S.P., Asner G., Cleveland C., Green P.A., Holland E., Karl D.M., Michaels A.F., Porter J., Townsend A. and Vorosmarty C.J. 2003. Global and regional nitrogen cycles: past, present and future. Biogeochemistry (submitted).

Goolsby D.A. and Battaglin W.A. 2001. Long-term changes in concentrations and flux of nitrogen in the Mississippi River Basin, USA. Hydrol. Process 15(7): 1209–1226.

Hession W.C., McBride M. and Bennett M. 2000. Statewide non-point-source pollution assessment methodology. J. Water Res. PL-ASCE 126(3): 146–155.

Hobbie J.E. (ed) 2000. Estuarine Science: A Synthetic Approach to Research and Practice. Island Press, Washington, DC, 539 pp.

Hopkinson C.S. and Vallino J.J. 1995. The relationships among mans activities in watersheds and estuaries – a model of runoff effects on patterns of estuarine community metabolism. Estuaries 18(4): 598–621.

Howarth R.W. 1998. An assessment of human influences on fluxes of nitrogen from the terrestrial landscape to the estuaries and continental shelves of the North Atlantic Ocean. Nutr. Cy. Agroecosyst. 52(2–3): 213–223.

Howarth R.W., Billen G., Swaney D., Townsend A., Jaworski N., Lajtha K., Downing J.A., Elmgren R., Caraco N., Jordan T., Berendse F., Freney J., Kudeyarov V., Murdoch P. and Zhu Z.L. 1996. Regional nitrogen budgets and riverine N&P fluxes for the drainages to the North Atlantic Ocean: natural and human influences. Biogeochemistry 35(1): 75–139.

Howarth R.W., Boyer E.W., Pabich W.J., andGalloway J.N. 2002. Nitrogen use in the United States from 1961–2000 and potential future trends. AMBIO 31(2): 88–96.

Jaworski N.A., Howarth R.W. and Hetling L.I. 1997. Atmospheric deposition of nitrogen oxides onto the landscape contributes to coastal eutrophication in the northeast United States. Environ. Sci. Technol. 31(7): 1995–2004.

Jordan T.E., Correll D.L. and Weller D.E. 1997. Nonpoint source discharges of nutrients from Piedmont watersheds of Chesapeake Bay. J. Am. Water Resour. As. 33(3): 631–645.

Justic D., Rabelais N.N., Turner R.E. and Dortch Q. 1995. Stoichiometric nutrient balance and origin of coastal eutrophication. Marine Pollut. Bull. 30: 41–46.

Kroeze C. and Seitzinger S.P. 1998. The impact of land use on N2O emissions from watersheds draining into the Northeastern Atlantic Ocean and European Seas. Environ. Pollut. 102(Suppl.): 149–158

Lerman A., Imboden D.M. and Gat J.R. 1995. Physics and Chemistry of Lakes. Springer-Verlag, Berlin and Heidelberg GmbH and Co. KG.

Lerner J., Matthews E. and Fung I. 1988. Methane emissions from animals: a global high-resolution data base. Global Biogeochem. Cy., 2: 139–156.

Leopold L.B., Wolman M.G. and Miller J.P. 1964. Fluvial Processes in Geomorphology. Freeman, New York.

Ludwig W. and Probst J.L. 1996. Predicting the oceanic input of organic carbon by continental erosion. Global Biogeochem. Cy. 10: 23–41.

Ludwig W. and Probst J.L. 1998. River sediment discharge to the oceans: present-day controls and global budgets. Am. J. Sci. 298: 265–295.

Mackenzie F.T., Ver L.M., Sabine C., Lane M. and Lerman A. 1993. C, N, P, S biogeochemical cycles and modeling of global change. In: Wollast R., Mackenzie T., Chou L. (eds) Interactions of C, N, P and S Biogeochemical Cycles and Global Change. NATO ASI Series I, 4, Springer-Verlag, New York, pp. 1–62.

McEvedy C. and Jones R. 1978. Atlas of World Population History. Penguin, New York.

Melillo J.M., McGuire A.D., Kicklighter D.W., Moore III B., Vörösmarty C.J. and Schloss A.L. 1993. Global climate change and terrestrial net primary production. Nature 363: 234–240.

Meybeck M. 1993. Riverine transport of atmospheric carbon – sources, global typology and budget. Water Air Soil Pollut. 70(1–4): 443–463.

Meybeck M. 1995. Global distribution of lakes. In: Lerman A. (ed) Physics and Chemistry of Lakes. Springer-Verlag, Berlin and Heidelberg GmbH and Co. KG.

Meybeck M. and Ragu A. 1995. River discharges to the Ocean: an assessment of suspended solids, major ions and nutrients. Laboratoire de Géologie Appliquée, Université P. et M. Curie, Paris, France.

Meybeck M. and Ragu A. 1997. River discharges to the oceans: an assessment of suspended solids, major ions, and nutrients.UNEP/WHO/GEMS-Water, 245 pp.

Meybeck M., Green P.A., andVörösmarty C.J. 2001. A new typology for mountains and other relief classes. An application to global continental water resources and population distribution. Mountain Res. Dev. 21(1): 34–45.

National Assessment Synthesis Team 2001. Climate Change Impacts on the United States: The Potential Consequences of Climate Variability and Change. Report for the US Global Change Research Program, Cambridge University Press, Cambridge, UK. http://www.usgcrp.gov/ or http://www.cambridge.org/.

National Research Council (NRC) 1985. Nutrient Requirements of Domestic Animals Series. Committee on Animal Nutrition. National Academy Press, Washington, DC.

Organization for Economic Co-Operation and Development (OECD) 1999. OECD Environmental Data – Compendium 1999, OECD, Paris.

Peterson B.J., Wollheim W.M., Mulholland P.J., Webster J.R., Meyer J.L., Tank J.L., Marti E., Bowden W.B., Valett M., Hershey A.E., McDowell W.H., Dodds W.K., Hamilton S.K., Gregory S. and Morrall D.D. 2001. Control of nitrogen export from watersheds by headwater streams. Science 292: 86–90.

Pionke H.B., Gburek W.J., Schnabel R.R., Sharpley A.N., andElwinger G.F. 1999. Seasonal flow, nutrient concentrations and loading patterns in stream flow draining an agricultural hill-land watershed. J. Hydrol. 220(1–2): 62–73.

Russell M.A., Walling D.E., Webb B.W. and Bearne R. 1998. The composition of nutrient fluxes from contrasting UK river basins. Hydrol. Process 12(9): 1461–1482.

Seitzinger S.P., Kroeze C., Bouwman A.F., Caraco N., Dentener F. and Stylkes R.V. 2002a. Global patterns of dissolved inorganic and particulate nitrogen inputs to coastal systems: recent conditions and future projections. Estuaries 25(4b): 640–655.

Seitzinger S.P., Styles R.V., Boyer E.W., Alexander R.B., Billen G., Howarth R.W., Mayer B. and van Breemen N. 2002b. Nitrogen retention in rivers: model development and application to watersheds in the northeastern USA. Biogeochemistry 57/58: 199–237.

Smil V. 1999. Nitrogen in crop production: an account of global flows. Global Biogeochem. Cy. 13: 647–662.

Steel E.W. and McGhee T.J. 1979. Water Supply and Sewerage. McGraw-Hill, New York.

Syvitski J.P., Morehead M.D., Bahr D.B. and Mulder T. 2000. Estimating fluvial sediment transport: the rating parameters. Water Resour. Res. 36(9): 2747–2760.

Turner R.E. and Rabelais N.N. 1994. Coastal eutrophication near the Mississippi river delta. Nature 368: 619–621

(UN-Habitat) United Nations Human Settlements Programme 2001. Global Urban Indicators Version 2 (Year of Reference – 1998). http://www.unhabitat.org/programmes/guo.

Van Dretch G., Bouwman A.F., Knoop J.M., Meinardi C. and Beusen A. 2001. Global pollution of surface waters from point and nonpoint sources of nitrogen. In: Optimizing Nitrogen Management in

Food and Energy Production and Environmental Protection: Proceedings of the 2nd International Nitrogen Conference on Science Policy The Scientific World 1(S2), pp. 632–641.

Ver L.M., Mackenzie F.T. and Lerman A. 1999. Carbon cycle in the coastal zone: effects of global perturbations and change in the past three centuries. Chem. Geol. 159: 283–304.

Vörösmarty C.J. and Meybeck M. 2003. Responses of continental aquatic systems at the global scale: new paradigms, new methods. In: Kabat P., Claussen M., Dirmeyer P.A., Gash J.H.C., Bravo de Guenni L., Meybeck M., Pielke Sr. R.A., Vörösmarty C.J., Hutjes R.W.A. and Lutkemeier S. (eds) Vegetation, Water, Humans and the Climate. IGBP BAHC, Potsdam, Germany, pp. 517–572.

Vörösmarty C.J. and Peterson B.J. 2000. Macro-scale models of water and nutrient flux to the coastal zone. In: Hobbie J.E. (ed) Estuarine Science: A Synthetic Approach to Research and Practice. Island Press, Washington, DC.

Vörösmarty C.J., Federer C.A. and Schloss A.L. 1998. Evaporation functions compared on US watersheds: Possible implications for global-scale water balance and terrestrial ecosystem modeling. J. Hydrol. 207(3–4): 147–169.

Vörösmarty C.J., Fekete B.M., Meybeck M. and Lammers R.B. 2000a. Global system of rivers: its role in organizing continental landmass and defining land-to-ocean linkages. Global Biogeochem. Cy. 14(2): 599–621.

Vörösmarty C.J., Fekete B.M., Meybeck M. and Lammers R.B. 2000b. Geomorphometric attributes of the global system of rivers at 30-minute spatial resolution. J. Hydrol. 237(1–2): 17–39.

Vörösmarty C.J., Green P.A., Salisbury J. and Lammers R.B. 2000c. Global water resources: vulnerability from climate change and population growth. Science 289: 284–288.

Wollheim W.M., Peterson B.J., Deegan L.A., Hobbie J.E., Hooker B., Bowden W.B., Edwardson K.J., Arscott D.B., Hershey A.E. and Finlay J. 2001. Influence of stream size on ammonium and suspended particulate nitrogen processing. Limnol. Oceanogr. 46(1): 1–13.

World Resources Institute (WRI) 1998. World Resources: A Guide to the Global Environment 1998–1999. World Resources Institute, Washington, DC.